*Journal of the European Ceramic Society* 7 (1991) 93–99

# Fabrication of Flaw-tolerant Aluminum-titanate-reinforced Alumina

Julie L. Runyan* & Stephen J. Bennison‡

Ceramics Division, National Institute of Standards and Technology, Gaithersburg, MD 20899, USA

(Received 18 June 1990; accepted 23 October 1990)

***Abstract***

*The fabrication and the flaw tolerance behavior of particulate aluminum-titanate-reinforced alumina composites have been studied. High-density (~99% theoretical) composites with controlled microstructures are readily produced via a conventional ceramics processing scheme using starting powders of α-alumina and β-aluminum titanate. Indentation-strength measurements demonstrate that these composites are highly flaw tolerant. Direct observations of crack evolution from Vickers indentations during loading reveal a strong crack-stabilization with pre-failure extensions of a millimeter or more. This stabilization gives rise to the flaw tolerance properties and results from pronounced crack-resistance (R-curve) behavior. Grain-localized crack bridging is active in these materials and is believed to be a contributor to the R-curve properties.*

*In dieser Arbeit wurde die Herstellung und die Anfälligkeit gegenüber Gefügefehlern eines $Al_2TiO_5$-Teilchen verstärkten $Al_2O_3$-Verbundwerkstoffs untersucht. Aus α-$Al_2O_3$- und β-$Al_2TiO_5$-Ausgangspulvern konnten mittels keramiktypischer Verfahrensweise Verbundwerkstoffe mit hoher Dichte (99% th.) und mit kontrollierten Gefügen auf einfache Weise gesintert werden. Härteeindruck- und Festigkeitsmessungen konnten zeigen, daß diese Verbundwerkstoffe eine sehr geringe Anfälligkeit gegenüber Gefügefehlern besitzen. Die in-situ Beobachtung der durch Vickers-Eindrücke hervorgerufenen Rißausbreitung während der Belastung zeigt eine hohe Rißstabilisierung mit Rißlängen von über 1 mm vor dem Versagen des Materials. Diese Stabilisierung vermindert die Anfälligkeit gegenüber Gefügefehlern und ist die Folge eines ausgeprägten R-Kurven-Verhaltens dieses Werkstoffs. Rißflankenüberbrückung durch Reibungsflächen an einzelnen Körnern kommt in diesen Materialien vor und wird als eine der Ursachen für das R-Kurven-Verhalten gesehen.*

*On a étudié l'élaboration et la tolérance aux défauts de composites d'alumine renforcée par des particules de titanate d'aluminium. On a pu ainsi produire des composites de haute densité (~99% de la densité théorique) à microstructure contrôlée, et ceci par un procédé d'élaboration conventionnelle mettant en jeu des poudres de départ d'alumine α et de titanate d'aluminium β. Des mesures de résistance à la rupture par indentation ont montré que ces composites sont hautement résistants aux défauts. Les observations directes d'évolution sous charge de fissures induites par indentation Vickers ont révélé une forte stabilisation des fissures avec des extensions de pré-fissuration d'un millimètre ou plus. Cette stabilisation entraîne les propriétés de tolérance aux défauts et est la conséquence d'une haute résistance à la fissuration (courbe R). On suppose que le pontage des fissures observé pour les grains contribue également aux propriétés des courbes R.*

## 1 Introduction

One of the more important consequences of an increasing crack resistance with increasing crack length (*R*-curve, *T*-curve) behavior[1–9] in ceramics is the reduced sensitivity of the strength to the size of any processing or service-induced defects, viz. the

* Present address: Department of Materials Engineering, Virginia Polytechnic Institute and State University, Blacksburg, VA 24061, USA.
‡ To whom correspondence should be addressed at: Department of Materials Science and Engineering, Lehigh University, Bethlehem, PA 18015, USA.



*Journal of the European Ceramic Society* 0955-2219/91/$3.50 

quality of 'flaw tolerance'.[5,10,11] The resulting improvements in reliability as reflected in greater Weibull moduli[12-16] and enhanced fatigue limits[17] make flaw tolerance a desirable property for brittle materials in structural applications.

A variety of phenomena can give rise to *R*-curves in ceramics.[18] For non-transforming materials with relatively simple microstructures and with predominantly intergranular fracture, grain-localized crack bridging has been identified as a primary mechanism.[19,20] In this case, intact grains bridge the crack walls and apply closure forces that shield the crack tip from the applied stress intensity field.[21,22] These bridging grains are assumed to be 'locked' into the microstructure by local thermal expansion anisotropy stresses.[8,23] The important microstructural and material parameters include grain size and shape, the intensity of the residual stress, grain boundary toughness and friction at the sliding grain–matrix interface.[23] A proper understanding of the role of these parameters opens the way to tailoring the *R*-curve and flaw-tolerance properties through controlled processing.[24]

In the present study, improvements in the *R*-curve and flaw-tolerance characteristics of alumina are sought through enhancement of the local residual stress levels. The approach is to incorporate a second phase $\beta$-aluminum titanate into the $\alpha$-alumina matrix. Aluminum titanate exhibits extremely high thermal expansion anisotropy;[25] when added to alumina it is expected to raise the maximum levels of residual stress by approximately one order of magnitude. This estimate is determined from $\sigma_R \simeq \frac{1}{2}E\Delta\alpha\Delta T$ and the most severe misorientation of alumina and aluminum titanate; ($\sigma_R$ = residual stress; $E$ = Young's modulus, $\Delta\alpha$ = thermal expansion difference, $\Delta T$ = temperature range over which stresses develop).

The fabrication of aluminum titanate and alumina–aluminum titanate is usually accomplished via a reaction-sintering route with starting powders of alumina and titania.[26-29] However, unless careful control of the powder characteristics is maintained during processing[30] the resulting microstructures generally display low as-fired densities (<90% theoretical) and abnormal grain growth, making them weak and, therefore, generally unsuitable for structural applications.

In the present work a conventional ceramics processing scheme using starting powders of alumina and aluminum titanate is developed whereby composites of high fired density and controlled grain structure are readily manufactured. The *R*-curve and flaw-tolerance properties are investigated using the indentation–strength technique in which the strength is determined as a function of indentation load.[5,9,11,22] The interaction of cracks with the microstructure is studied using a statically loaded biaxial flexure device mounted either in an optical or scanning electron microscope (SEM). It will be shown that certain composites of $\alpha$-alumina reinforced with $\beta$-aluminum titanate demonstrate pronounced flaw tolerance resulting from the crack-stabilizing effect of a strong *R*-curve. The unusual flaw-tolerance properties coupled with the ease of fabrication make these composites attractive for applications where components are subjected to damage during service.

## 2 Experimental

### 2.1 Composite fabrication

All powder processing was carried out in class A-100 clean room conditions. A stable colloidal suspension of high-purity $\alpha$-$Al_2O_3$ (Sumitomo AKP-HP grade (99·995% pure, 0·5 $\mu$m crystallites), Sumitomo Chemical America Inc., New York, USA) in water containing the desired volume fraction of $\beta$-$Al_2TiO_5$ (99·9%, 1–5 $\mu$m particle size, Trans-Tech Inc., Adamstown, USA) was prepared by adjusting the pH to $\approx$3 with additions of $HNO_3$. Drying was carried out using a hot-plate while stirring continuously and the resulting cake was subsequently broken down by crushing in a polyethene bag. Disc-shaped test specimens, 25 mm diameter and 5 mm thickness, were fabricated by uniaxial pressing at 63 MPa using a high-purity graphite die, punch and spacer assembly. Removal of any defects associated with die pressing was achieved by subsequent wet-bag isostatic pressing at 350 MPa. A green density of $\approx$55% of the theoretical limit was attained using this procedure.

Green discs were packed in loose alumina powder in high-purity alumina crucibles for firing using a two-stage heat treatment. The first stage consisted of heating at a rate of 50°C/h to a calcining temperature of 1050°C with a 12 h soak. The second stage consisted of heating at a rate of 500°C/h from the calcining temperature to a sintering temperature of 1600°C with hold times of 1 h and 16 h. Specimens were cooled at $\approx$500°C/h. All heat treatments were carried out in air using a $MoSi_2$ resistance-heated furnace.

Sample specimens from each batch were subjected to microstructural characterization. Densities were measured by the Archimedes method using water as the immersion medium.[31] Surfaces were prepared,

where possible, for optical and scanning electron microscopy (SEM) by diamond-polishing to a 1 $\mu$m finish. Microstructures were revealed by thermal etching (air, 1500°C, 6 min) and grain sizes were determined by a linear intercept technique.[32] Where polishing was found to be impractical due to localized spontaneous microfracture, approximate grain sizes were determined from fracture surfaces examined by SEM. Phases present in the composite were identified by X-ray diffraction.

### 2.2 Indentation–strength testing

Prior to testing, each fired disc was machined to a thickness of 2·5 mm and the prospective tensile face diamond-polished to a 1 $\mu$m finish. Care was taken to ensure that polishing removed the majority of the surface damage introduced during the preliminary machining operation. Most specimens were indented at their face centers with a Vickers diamond pyramid at contact loads between 3 and 300 N; some discs were left unindented as controls. All indentations were made under ambient laboratory conditions and allowed to stand for 10 min. Biaxial strength tests were then made using a flat circular punch (4 mm diameter) and a three-point support (15 mm diameter).[33] A drop of dry silicone oil was placed on each indentation prior to testing and the failure times were kept below 20 ms to minimize possible effects from moisture assisted non-equilibrium crack growth. Inert strengths were calculated from the breaking loads and specimen dimensions using thin-plate formulas.[34] Special effort was made to examine all specimens after testing using optical microscopy to verify that the indentation contact site acted as the origin of failure. Unsuccessful breaks were incorporated into the data pool of unindented controls.

Direct observations of crack extension from indentations during loading were made on selected specimens using a biaxial flexure device mounted on an optical microscope.[19] Crack–microstructure interactions were also investigated using this fixture mounted in an SEM.

## 3 Results

Table 1 lists the salient characteristics of the two composites (20 vol.% aluminum titanate) prepared in this study.

Figure 1 shows the microstructure of composite A (alumina grain size = 5·8 $\mu$m). The aluminum titanate phase is primarily distributed as isolated particles both at grain boundaries and within grains.

**Table 1.** Microstructural characteristics of the two composites studied

| *Composite* | *Volume % $Al_2TiO_5$* | *Grain size $Al_2O_3$ ($\mu$m)* | *Density (mg $m^{-3}$)* | *Phases present* |
|---|---|---|---|---|
| A | 20 | 5·8 | 3·88 (98·9%) | $\alpha$-$Al_2O_3$ $\beta$-$Al_2TiO_5$ |
| B | 20 | $\approx$14 | 3·89 (99·0%) | $\alpha$-$Al_2O_3$ $\beta$-$Al_2TiO_5$ |

Local concentrations of aluminum titanate are occasionally observed. These islands typically consist of 5–10 grains and are probably remnants of hard agglomerates in the base powder. The alumina matrix shows no sign of abnormal grain growth although facetted grain shapes are evident. The microstructure is of high density ($\sim$99%), as confirmed by direct measurements (Table 1), with angular pores resulting from grain pullout during polishing constituting the prominent surface defect population. Microcracks are seen in this composite and are predominantly associated with the islands of aluminum titanate.

Figure 2 shows the microstructure of composite B (alumina grain size $\approx$ 14 $\mu$m). The primary distinctions between composites A and B are the increased scale of the microstructure in the latter and the widespread occurrence of microcracking in this coarser material. The difficulty in preparing quality polished sections for microscopy implies that the majority of the microcracks form spontaneously on cooling from the sintering temperature.

Figure 3 presents the measured inert strengths as a function of indentation load for both materials. Each datum point represents the mean and standard

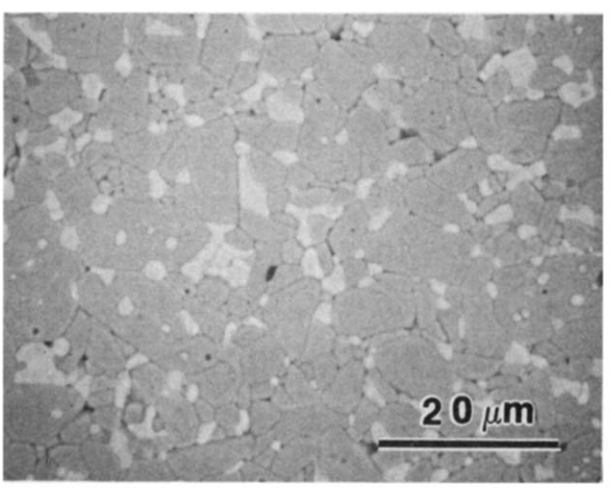


**Fig. 1.** SEM micrograph (back-scattered electron image) of a polished and etched section from composite A (20 vol.% $Al_2TiO_5$, $Al_2O_3$ grain size = 5·8 $\mu$m). The lighter phase is $Al_2TiO_5$, the gray phase is $Al_2O_3$ and the black phase is porosity.

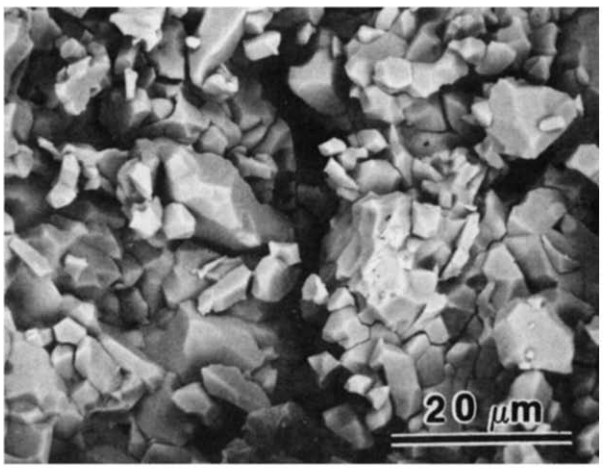


Fig. 2. SEM micrograph (back-scattered electron image) of a fracture surface from composite B (20 vol.% $Al_2TiO_5$, $Al_2O_3$ grain size $\approx 14\,\mu m$).

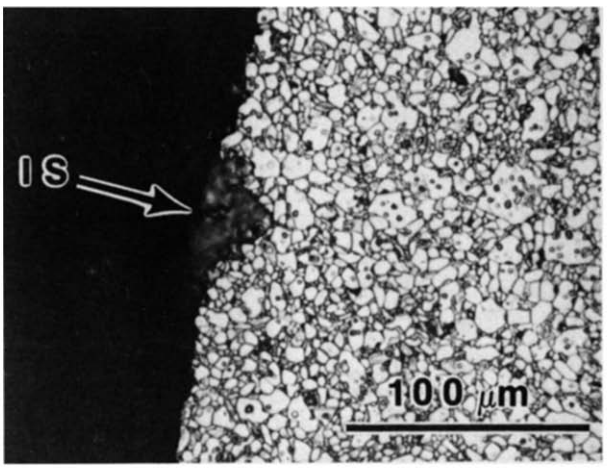


Fig. 4. Optical micrograph (reflected light) of fracture path (*post mortem*) in composite A. The 30 N indentation site (IS) is clearly included in the fracture path.

deviation of, on average, four indentation–flaw failures; the boxes at the far left represent failures from natural flaws. Figure 4 is a post-mortem micrograph showing the fracture path in one specimen tested; the fracture clearly includes the indentation site and is assumed to have initiated from it. Great care was taken to ensure the indentation site was the source of the critical flaw for *all* data reported.

Both materials show *unusually* pronounced flaw tolerance behavior with little dependence of the strength on indentation load. The strengths of specimens containing 300 N indentations are only slightly degraded ($\approx 8\%$) in comparison to the unindented controls. Composite B is considerably weaker, by a factor of $\approx 5$, than composite A for a relatively small ($\approx 2{\cdot}5$) increase in grain size.

Observations of crack evolution from an indentation during static loading are presented in Figs 5 and 6. Figure 5 shows the crack pattern from a 30 N indentation during subsequent biaxial tensile loading. The radial cracks have extended stably from an initial size of the order of $100\,\mu m$ to sizes in the millimeter range. Note that the cracks are in equilibrium with the applied tensile field. Figure 6 shows interactions of the primary radial crack with features of the microstructure. The failure mode is predominantly intergranular and active bridging can be readily observed. The primary crack is heavily deflected on the scale of the grain size and tends to be attracted to the matrix–second-phase interface.

Figure 7 shows a secondary crack of 5–20 grain dimensions in size formed during the loading of composite A. Such secondary cracks are seen on the tensile surface of the test specimen within the zone of

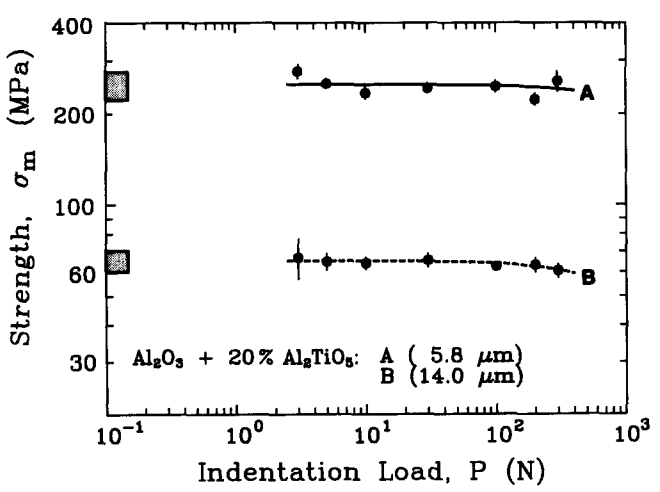


Fig. 3. Plot of inert strength, $\sigma_m$, versus indentation load, $P$, for the two composites. The curves are empirical linear fits to the data and serve only as a guide to the eye. Note the pronounced flaw tolerance of these materials.

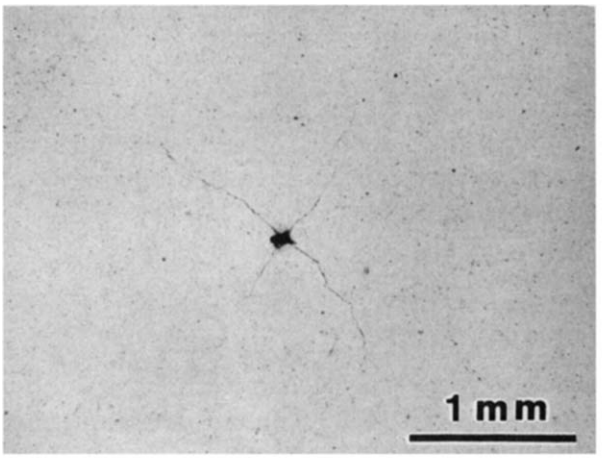


Fig. 5. Optical micrograph (reflected light) of a 30 N indentation loaded in equibiaxial flexure (composite A). The radial cracks have grown *stably* from the initial size ($\sim 100\,\mu m$) produced by indentation and are in equilibrium with the applied tensile field.

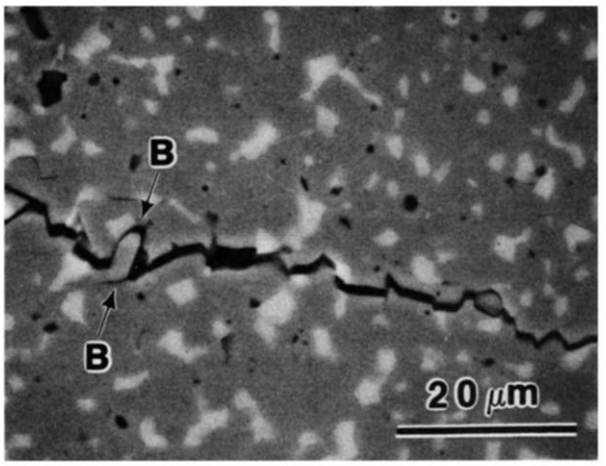


**Fig. 6.** SEM micrograph (back-scattered electron image) showing details of crack–microstructure interactions. Evidence for bridging grains can be seen (e.g. at B–B).

constant equibiaxial tension. The location of these cracks does not appear to correlate with the position and evolution of the primary cracks developing from the indentation site.

Figure 8 displays the load versus displacement of the testing machine cross-head responses for the two composites each containing 200 N Vickers indentations. The finer material (A) shows predominantly linear (Hookean) behavior during loading with slight non-linear characteristics just prior to peak load. The composite fails abruptly at peak load. The coarser material (B) shows very pronounced non-linear behavior with greater strain to a lower maximum in load. Failure then proceeds in a stable manner until final rupture at very large displacements (strains). Widespread secondary cracking is observed on the tensile face of composite B during testing. Note that a finite force, $P'$, is required to separate the crack walls of composite B after large displacements.

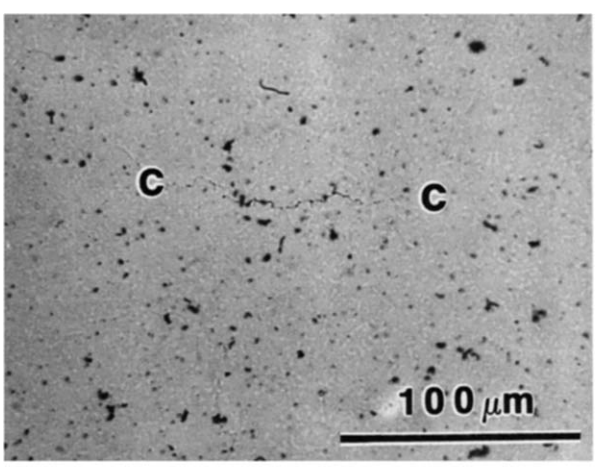


**Fig. 7.** Optical micrograph (reflected light) of a secondary crack (C–G) located on the tensile face of one test specimen within the equibiaxial tensile zone.

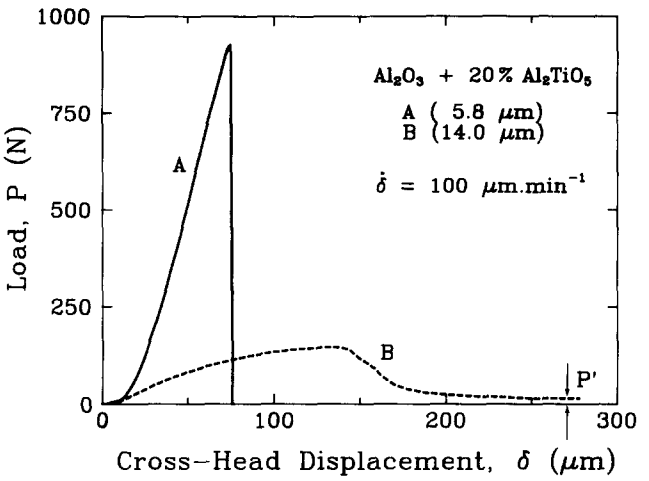


**Fig. 8.** Load versus cross-head displacement traces for composites A and B each containing 200 N Vickers indentations. Material A displays unstable fracture at a critical displacement and evidence of slight non-linearity prior to reaching peak load. Material B shows stable fracture and very pronounced non-linear behavior. Note material B show some load bearing capacity well after peak loading (denoted by $P'$).

## 4 Discussion

Two important conclusions may be drawn from these experiments: (i) high-density alumina–aluminum-titanate composites with controlled microstructures can be readily fabricated via a processing route using starting powders of alumina and aluminum titanate; (ii) reinforcement of alumina with aluminum titanate results in composites with pronounced flaw tolerance.

The microstructures developed in the present work display several improvements over those generally produced by reaction sintering between alumina and titania.[26–29] The first clear improvement is the absence of abnormal grain growth and associated pore–grain boundary separation. Addition of the aluminum titanate phase prior to the start of sintering is thought to suppress the initiation of abnormal grains by a pinning mechanism similar to that suggested for other two-phase systems.[35] The second improvement is the attainment of high (~99% theoretical) fired densities. The high density results from the avoidance of pore–grain boundary separation associated with abnormal grain growth[36] and the indirect enhancement of densification with respect to coarsening resulting from grain growth inhibition.[37] Also, it is possible that the aluminum titanate enhances densification processes directly in a fashion analogous to the function of titania additions to alumina.[38,39]

The indentation–strength properties of the composites may be compared with those of unreinforced aluminas of varying $R$-curve and flaw tolerance

characteristics. Figure 9 presents the behavior of composite A together with trends for aluminas with grain sizes of 5·8 and 80 $\mu$m. (The trends for the aluminas were calculated from a 'calibrated' grain-bridging model used previously to interpret the effect of grain size on *R*-curve behavior.[23,24]) It can be seen that composite A has superior flaw tolerance to the 80 $\mu$m alumina (D), i.e. it is stronger and displays less degradation in strength with increasing contact load. The remaining alumina (C), with comparable grain size to composite A, shows higher strengths at lower indentation loads but the strength degrades rapidly with increasing contact load and eventually falls well below composite A at the highest loads. Composite A is, therefore, a better choice of material than monophase alumina for applications where the component is subjected to in-service damage.

The composites may also be compared to pure aluminum titanate ceramics. It is generally difficult to fabricate aluminum titanate with sufficiently fine grain size to avoid spontaneous microcracking on cooling from the sintering temperature.[26-29] As such, it is damage tolerant and shows strong *R*-curve behavior but at the same time is weak (strengths $\approx$20 MPa for optimum load–displacement characteristics).[40] Composite B displays similar load versus cross-head displacement properties to pure aluminum titanate, is equally damage tolerant but is stronger by approximately a factor of three. Composite B may, therefore, be considered a contender for applications where pure aluminum titanate is presently used.

The unusual flaw tolerance of the aluminum-titanate-reinforced alumina composites results from strong stabilization of incipient critical flaws; *this stabilization is a manifestation of pronounced R-curve behavior.* The underlying physical mechanism(s) giving rise to the flaw-tolerance properties observed are yet to be unequivocally identified. Evidence for grain bridging is presented in the form of in-situ observations of loaded cracks (Fig. 6). The ability of composite B to support a finite load even after what is normally considered catastrophic failure (Fig. 8) further suggests the presence of intact grain bridges across the crack–wall interfaces. These preliminary observations imply that grain bridging is a contributor to the *R*-curve and flaw-tolerance properties of the composites.

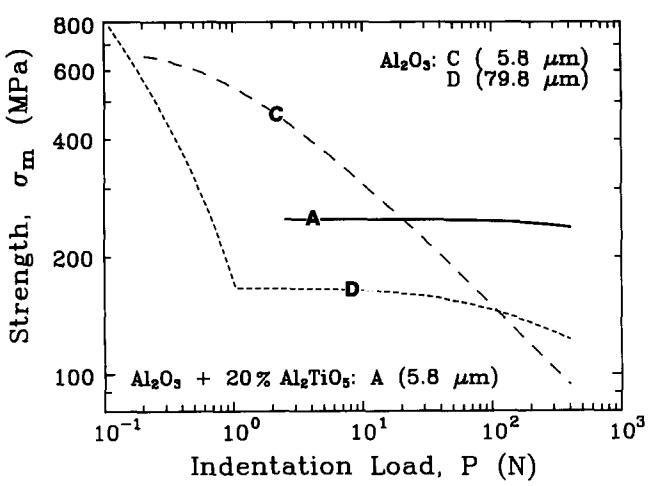


**Fig. 9.** Strength, $\sigma_m$, versus indentation load, *P*, characteristics. Results for composite A compared to trends calculated for aluminas of grain sizes C, 5·8 $\mu$m; D, 79·8 $\mu$m using a bridging model.[23,24]

The subsidiary cracking observed on the tensile faces of the test specimens is also expected to contribute to the damage tolerance of the composites. One consequence of the subsidiary cracking is a non-linear stress–strain response as reflected in the load–deflection traces recorded (Fig. 8). Such non-linear behavior influences the strength properties by reducing the applied stress-intensity field.[41,42] The mechanism through which the composites tolerate widespread damage evolution is presently unclear. However, considering the potential benefits of such unusual damage-tolerant characteristics further investigation is warranted. It is worth noting that the behavior observed in the present work is similar to damage phenomena reported for some continuous fiber-reinforced composites.[43]

It is anticipated that the strength and damage-tolerance properties of alumina–aluminum titanate composites can be further tailored through microstructure adjustment. When manipulating the toughness behavior in this manner there is a compromise between the component strength and flaw tolerance. Potential applications will ultimately depend on a foreknowledge of the degree of damage a component is likely to experience and the stresses to be supported. It is recommended that $Al_2O_3$–$Al_2TiO_5$ composites are given full consideration for components where damage tolerance and reliability are the primary design requirements.

## Acknowledgements

The authors wish to thank E. P. Butler, B. R. Lawn, N. P. Padture and J. Rödel for useful discussions. J. F. Kelly contributed to the SEM work, J. Cline assisted with the X-ray diffraction characterization and S. Darby machined the test specimens. The work was supported by the US Air Force Office of Scientific Research and E. I. DuPont de Nemours & Co. Inc.

## References


1. Hübner, H. & Jillek, W., Sub-critical crack extension and crack resistance in polycrystalline alumina. *J. Mater. Sci.*, **12** (1977) 117–25.
2. Knehans, R. & Steinbrech, R. W., Memory effect of crack resistance during slow crack growth in notched $Al_2O_3$ bend specimens. *J. Mater. Sci. Lett.*, **1** (1982) 327–9.
3. Steinbrech, R. W., Knehans, R. & Schaarwächter, W., Increase of crack resistance during slow crack growth in $Al_2O_3$ bend specimens. *J. Mater. Sci.*, **18** (1983) 265–70.
4. Knehans, R. & Steinbrech, R. W., Effect of grain size on the crack-resistance curves of $Al_2O_3$ bend specimens. In *Science of Ceramics*, Vol. 12, ed. P. Vincenzini. Ceramurgia, Imola, Italy, 1984, pp. 613–19.
5. Cook, R. F., Lawn, B. R. & Fairbanks, C. J., Microstructure–strength properties in ceramics. I. Effect of crack size on toughness. *J. Am. Ceram. Soc.*, **68** (1985) 604–15.
6. Cook, R. F., Lawn, B. R. & Fairbanks, G. J., Microstructure–strength properties in ceramics: II. Fatigue relations. *J. Am. Ceram. Soc.*, **68** (1985) 616–23.
7. Rose, L. R. F. & Swain, M. V., Two *R*-curves for partially stabilized zirconia. *J. Am. Ceram. Soc.*, **69** (1986) 203–7.
8. Swain, M. V., *R*-curve behavior in a polycrystalline alumina material. *J. Mater. Sci. Lett.*, **5** (1986) 1313–15.
9. Krause, R. F., Fuller, E. R. & Rhodes, J. F., Fracture resistance behavior of silicon carbide whisker-reinforced alumina composites with different porosities. *J. Am. Ceram. Soc.*, **73** (1990) 559–66.
10. Lawn, B. R. & Fairbanks, C. J., Toughness and flaw responses in nontransforming ceramics: implications for NDE. In *Review of Progress in Quantitative NDE*, Vol. 6B, ed. D. O. Thompson & D. E. Chimenti. Plenum, NY, USA, 1987, pp. 1023–30.
11. Bennison, S. J. & Lawn, B. R., Flaw tolerance in ceramics with rising crack-resistance behavior. *J. Mater. Sci.*, **24** (1989) 3169–75.
12. Kendall, K., McN. Alford, N., Tan, S. R. & Birchall, J. D., Influence of toughness on Weibull modulus of ceramic bending strength. *J. Mater. Res.*, **1** (1986) 120–3.
13. Cook, R. F. & Clarke, D. R., Fracture stability, *R*-curves and strength variability. *Acta Metall.*, **36** (1988) 555–62.
14. Shetty, D. K. & Wang, J-S., Crack stability and strength distribution of ceramics that exhibit rising crack-growth-resistance (*R*-curve) behavior. *J. Am. Ceram. Soc.*, **72** (1989) 1158–62.
15. Evans, A. G., New opportunities in the processing of high reliability structural ceramics. In *Ceramic Transactions*, Vol. 1, ed. G. L. Messing, E. R. Fuller, Jr & H. Hausner. American Ceramic Society, Westerville, OH, USA, 1989, pp. 989–1010.
16. Li, C-W. & Yamanis, J., Super-tough silicon nitride with *R*-curve behavior. *Ceramic Engineering and Science Proceedings*, ed. R. E. Barks. The American Society, Westerville OH, USA, **10** (1989) 632–45.
17. Lathabai, S. & Lawn, B. R., Fatigue limits in noncyclic loading of ceramics with crack-resistance curves. *J. Mater. Sci.*, **24** (1989) 4298–306.
18. Evans, A. G., Perspectives on the development of high-toughness ceramics. *J. Am. Ceram. Soc.*, **73** (1990) 187–206.
19. Swanson, P. L., Fairbanks, C. J., Lawn, B. R., Mai, Y-W. & Hockey, B. J., Crack-interface grain bridging as a fracture resistance mechanism in ceramics. I. Experimental study on alumina. *J. Am. Ceram. Soc.*, **70** (1987) 279–89.
20. Swanson, P. L., Crack-interface traction: A fracture-resistance mechanism in brittle polycrystals. In *Advances in Ceramics*, Vol. 22. American Ceramic Society, Westerville, OH, USA, 1988, pp. 135–55.
21. Mai, Y-W. & Lawn, B. R., Crack-interface grain bridging as a fracture resistance mechanism in ceramics. II. Theoretical Fracture Mechanics Model. *J. Am. Ceram. Soc.*, **70** (1987) 289–94.
22. Cook, R. F., Fairbanks, C. J., Lawn, B. R. & Mai, Y-W., Crack resistance by interfacial bridging: Its role in determining strength characteristics. *J. Mater. Res.*, **2** (1987) 345–56.
23. Bennison, S. J. & Lawn, B. R., Role of interfacial grain-bridging sliding friction in the crack-resistance and strength properties of nontransforming ceramics. *Acta Metall.*, **37** (1989) 2659–71.
24. Chantikul, P., Bennison, S. J. & Lawn, B. R., Role of grain size in the strength and *R*-curve properties of alumina. *J. Am. Ceram. Soc.*, **73** (1990) 2419–27.
25. Bayer, G., Thermal expansion characteristics and stability of pseudobrookite type compounds, $M_3O_5$. *J. Less Common Met.*, **24** (1971) 129–38.
26. Cleveland, J. J. & Bradt, R. C., Grain size/microcracking relations for pseudobrookite oxides. *J. Am. Ceram. Soc.*, **61** (1978) 478–81.
27. Hamano, K., Ohya, Y. & Nakagawa, Z-E., Microstructure and mechanical strength of aluminum titanate ceramic prepared from mixture of alumina and titania. *Yogyo-Kyokai-Shi*, **91** (1983) 95–101.
28. Ohya, Y., Hamano, K. & Nakagawa, Z-E., Microstructure and mechanical strength of aluminum titanate ceramics prepared from synthesized powders. *Yogyo-Kyokai-Shi*, **91** (1983) 289–97.
29. Qian, D-F., Ohya, Y., Hamano, K. & Nakagawa, Z-E., Effects of excess alumina on microstructure of aluminum titanate ceramics prepared from mixture of alumina and titania. *Yogyo-Kyokai-Shi*, **93** (1985) 315–21.
30. Okamura, H., Barringer, E. A. & Bowen, H. K., Preparation and sintering of narrow-sized $Al_2O_3$–$TiO_2$ composites. *J. Mater. Sci.*, **24** (1989) 1867–80.
31. Pennings, E. C. M. & Grellner, W., Precise nondestructive determination of the density of porous ceramics. *J. Am. Ceram. Soc.*, **72** (1989) 1268–70.
32. Wurst, J. C. & Nelson, J. A., Lineal intercept technique for measuring grain size in two-phase polycrystalline ceramics. *J. Am. Ceram. Soc.*, **55** (1972) 109.
33. Marshall, D. B., An improved biaxial flexure test for ceramics. *Am. Ceram. Soc. Bull.*, **59** (1980) 551–3.
34. De With, G. & Wagemans, H. H. M., Ball-on-ring test revisited. *J. Am. Ceram. Soc.*, **72** (1989) 1538–41.
35. Brook, R. J., Controlled grain growth. In *Treatise on Materials Science and Technology*, Vol. 9, ed. F. F. Y. Wang. Academic Press, NY, USA, 1976, pp. 331–64.
36. Coble, R. L. & Burke, J. E., Sintering in ceramics. *Progr. Ceram. Sci.*, **3** (1963) 197–251.
37. Harmer, M. P., Use of solid-solution additives in ceramic processing. In *Advance in Ceramics*, Vol. 10, ed. W. D. Kingery. American Ceramic Society, Westerville, OH, USA, 1984, pp. 679–96.
38. Bagley, R. D., Cutler, I. B. & Johnson, D. L., Effect of $TiO_2$ on initial sintering of $Al_2O_3$. *J. Am. Ceram. Soc.*, **53** (1970) 136–41.
39. Morgan, P. E. D. & Koutsoutis, M. S., Phase studies concerning sintering in aluminas doped with $Ti^{4+}$. *J. Am. Ceram. Soc.*, **68** (1985) C156–C158.
40. Hamano, K., Ohya, Y. & Nakagawa, Z-E., Crack propagation resistance of aluminum titanate ceramics. *Int. J. High Technol. Ceram.*, **1** (1985) 129–37.
41. Marshall, D. B., Strength characteristics of transformation-toughened zirconia. *J. Am. Ceram. Soc.*, **69** (1986) 173–80.
42. Chuang, T-J. & Mai, Y. W., Flexural behavior of strain-softening solids. *Int. J. Solids Structures*, **25** (1989) 1427–43.
43. Roach, D. A., Damage evolution in ceramic matrix composites. Paper 101-SIV-90 presented at the 92nd Annual Meeting of the American Ceramic Society, Dallas, TX, USA, 1990.